ELSEVIER

Journal of Nuclear Materials 307–311 (2002) 367–373

journal of nuclear materials

www.elsevier.com/locate/jnucmat

Effect of solute atoms on swelling in Ni alloys and pure Ni under He^+ ion irradiation

E. Wakai [a,*], T. Ezawa [b], J. Imamura [c], T. Takenaka [d], T. Tanabe [e], R. Oshima [f]

[a] *Department of Materials Science, Japan Atomic Energy Research Institute, Tokai, Nakagunn, Ibaraki 319-1195, Japan*
[b] *Faculty of System Engineering, University of East Asia, 2-1 Ichnomiya-gakuencho, Shimonoseki 751-8503, Japan*
[c] *Sumitomo Metal Co. Ltd., Amagasaki-city, Hyogo 660-0891, Japan*
[d] *Sumitomo Bakelite Co. Ltd., Nishi-ku, Kobe-city, Hyogo 651-2241, Japan*
[e] *Center for Integrated Research in Science and Engineering, Nagoya University, Furo-cho, Chikusa-ku, Nagoya 464-8603, Japan*
[f] *RIAST, Osaka Prefecture University, 1-2 Gakuen-cho, Sakai-city, Osaka 593, Japan*

Abstract

The effects of solute atoms on microstructural evolutions have been investigated using Ni alloys under 25 keV He^+ irradiation at 500 °C. The specimens used were pure Ni, Ni–Si, Ni–Co, Ni–Cu, Ni–Mn and Ni–Pd alloys with different volume size factors. The high number densities of dislocation loops about 1.5×10^{22} m^{-3} were formed in the specimens irradiated to 1×10^{19} ions/m^2, and they were approximately equivalent, except for Ni–Si. The mean size of loops tended to increase with the volume size factor of solute atoms. In a dose of 4×10^{20} ions/m^2, the swelling was changed from 0.2% to 4.5%, depending on the volume size factors. The number densities of bubbles tended to increase with the absolute values of the volume size factor, and the swelling increased with the volume size factors. This suggests that the mobility of helium and vacancy atoms may be influenced by the interaction of solute atoms with them.

1. Introduction

Effects of alloying elements on the microstructural evolution have been reported to be very sensitive to the volume size of solute atoms, and the microstructural changes and segregation of solute atoms to grain boundaries and surface would induce the degradation of mechanical properties and corrosion-resistance. Understanding the role of alloying elements and helium atom produced by the (n, α) reaction on defect structural evolution is very important for the development of fusion reactor materials.

The microstructural changes of Ni alloys under electron irradiation [1], D^+ ion irradiation [2], neutron irradiation [3] were systematically investigated using a parameter of the volume size factor of solute atoms. The microstructural change in pure Ni irradiated by He^+ ions was previously studied [4]. The purpose of this study is to investigate the effects of solute atoms with different volume size factors and He atoms on the evolution of dislocation loops and bubbles in several kinds of Ni binary alloys under He^+ ion irradiation.

2. Experimental procedure

Pure Ni and binary Ni alloys containing Si, Mn, Pd, Nb and Au were used as samples. The solute atoms of binary Ni alloys were selected by considering volume sizes [5], as given in Table 1. Ni–5.0at.%Si, Ni–4.6at.%Mn, Ni–5.4at.%Pd, Ni–2.3at.%Nb and Ni–1.3at.%Au alloys were prepared by melting 99.99%

* Corresponding author. Tel.: +81-29 282 6563; fax: +81-29 282 5922.
E-mail address: wakai@realab01.tokai.jaeri.go.jp (E. Wakai).

0022-3115/02/$ - see front matter © 2002 Elsevier Science B.V. All rights reserved.
PII: S0022-3115(02)01192-3

Table 1
Volume size factors of solute atoms in Ni

Solute atoms in Ni	Si	Co	Cu	Mn	Pd	Nb
Volume size factor	−5.8	1.8	7.2	23.2	41.3	51.2

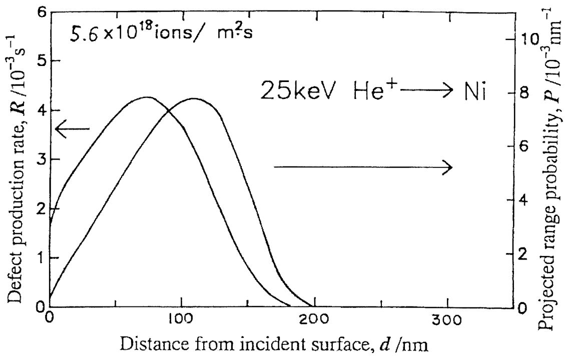

Fig. 1. Depth profiles of displacement damage rate and helium projected range probability in Ni irradiated by 25 keV He^{+} ions.

purity metals in a high-frequency induction furnace under high vacuum. After the solution heat treatment at 1100 °C, the ingots were cold-rolled down to sheets with a thickness of 0.06 mm and were again annealed at 1100 °C for 7.2×10^{3} s. The specimens were electro-polished at 4 V by the window method in a mixed solution of 60 vol.% sulfuric acid and 40 vol.% water at 15 °C. Additional polishing was done for Ni–Pd and Ni–Au alloys at 15 V in a mixed solution of 95 vol.% methanol and 5 vol.% perchloric acid at −33 °C. Ni–Mn alloys were polished at 15 V again in a mixed solution of 80 vol.% methanol and 20 vol.% perchloric acid at −33 °C.

The 25 keV He^{+} ion irradiation was performed at room temperature and 500 °C using an RF ion source. The depth profiles of displacement damage rate and implanted helium projected range probability are shown in Fig. 1. The temperature of 500 °C is the solid-solution region for all Ni alloys. The irradiations were performed with a flux of about 3×10^{18} He^{+}/m^{2} s to about 8×10^{21} He^{+}/m^{2} s. After the irradiation, the damage microstructures in the specimens were examined by a transmission electron microscope operated at 200 kV.

3. Results

Fig. 2(a)–(g) shows interstitial-type dislocation loops formed in pure Ni, Ni–5%Si, Ni–5%Co, Ni–5%Cu, Ni–5%Mn, Ni–5%Pd and Ni–2%Nb alloys, respectively, irradiated at 500 °C by 25 keV He^{+} ion with a dose of 1.0×10^{19} He^{+} ions/m^{2}. The micrographs were taken by a reflection of $g = 111$. The volume size of Si in Ni is −5.7%, and those of Ni–Co, Ni–Cu, Ni–Mn, Ni–Pd and Ni–Nb alloys for these solute atoms are +1.8%, +7.2%, +23.2%, +43.3% and +51.2%, respectively. The number density of loops in pure Ni and Ni alloys is approximately equivalent, except for the Ni–Si alloy. The mean diameters of dislocation loops in the specimens depended on the volume size factor of solute atoms, and it tended to increase with increasing the volume size factor. Many small dislocation loops with the diameter of about 4–6 nm were observed especially in Ni–Si alloy. The number density and mean diameter of dislocation loops are given in Fig. 3.

Figs. 4(a)–(c) and 5(a)–(c) show microstructures taken under low and high magnification, respectively, in

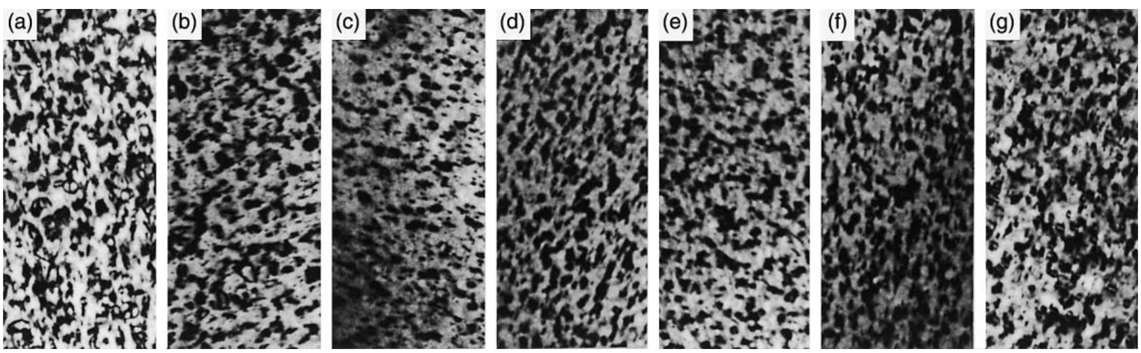

Fig. 2. Dislocation loops formed in (a) pure Ni, (b) Ni–5%Si, (c) Ni–5%Co, (d) Ni–5%Cu, (e) Ni–5%Mn, (f) Ni–5%Pd, (g) Ni–2%Nb irradiated at 500 °C by 25 keV He^{+} ions to a dose of 1×10^{19} ions/m^{2}.

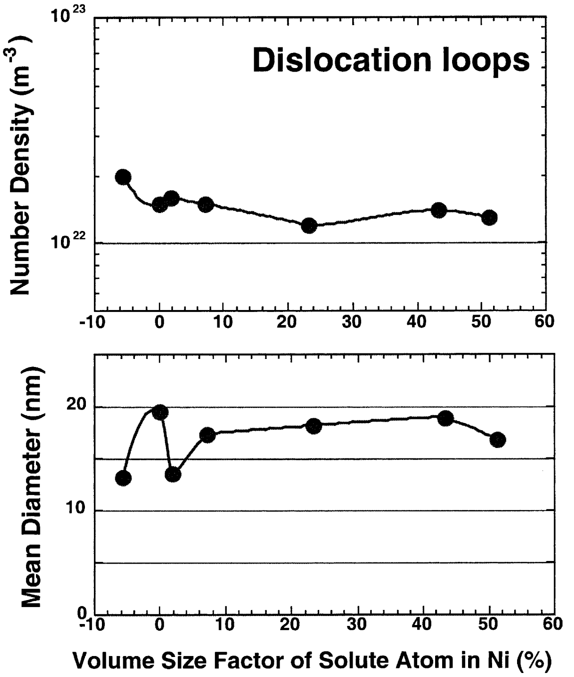

Fig. 3. The mean size and number density of dislocation loops formed in pure Ni and Ni alloys.

the Ni–9%Si, Ni–5%Co and Ni–5%Cu alloys irradiated at 500 °C to a dose of 4.1×10^{20} He^{+} ions/m^2 under a flux of 5.6×10^{18} ions/m^2 s for 73 s. A number of grown loops and bubbles were formed as seen in Fig. 4(a)–(c). The size of cavity formed in Ni–Si was smaller than that in the other alloys. Cavities were formed in matrix, on dislocation loops and at grain boundaries as seen in Fig. 5(a)–(c). In Fig. 6, bubbles formed in the pure Ni, Ni–5%Si, Ni–5%Mn and Ni–2%Nb alloys irradiated at 500 °C to a dose of 4.1×10^{20} He^{+} ions/m^2 under a flux of 3.2×10^{18} ions/m^2 s for 130 s. In the Ni–Si alloy, Ni_3Si precipitate was formed on the surface of bubbles. The relation between swelling and volume size factors is given in Fig. 7. The number density, mean size of bubbles and the swelling in the specimens irradiated at 500 °C to a dose of 4.1×10^{20}/m^2 are given in Table 2. The swelling tended to increase with increasing the volume size factors of solute atoms in Ni, while the number density of bubbles was increased with the absolute values of the volume size factors under a constant flux irradiation. The size of cavities in the specimens also tended to increase with the volume size factors, and the size of bubble in Ni–Si alloy was very small. Fig. 8 shows Ni_3Si precipitates formed on the surface of cavities in the matrix and around grain boundaries in the Ni–Si alloy. The growth of cavity in the Ni–Si matrix would be suppressed by the formation of precipitates.

4. Discussion

According to the study about the formation of dislocation loops in Ni alloys under 2 MeV electron irradiation, the density of dislocation loops formed at 500 °C was less than about 1×10^{21} m^{-3}, under a production rate of 2×10^{-3} dpa/s. The number density of loops formed in this study was about 1.5×10^{22} m^{-3} under He^{+} irradiation with a production rate of 7×10^{-3} dpa/s. Even in taking account of the facts that the nucleation of dislocation loops depends on the square root of the

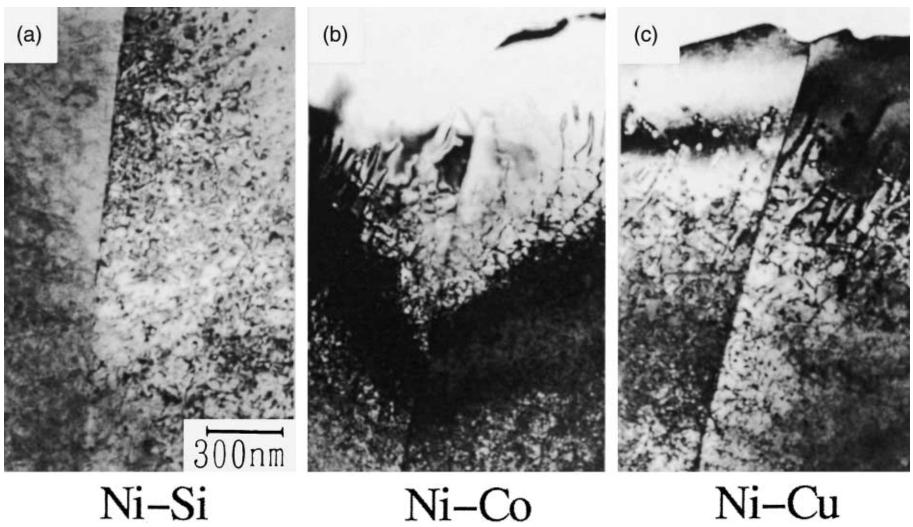

Fig. 4. Dislocation loops formed in Ni alloys irradiated at 500 °C to a dose of 4×10^{20} ions/m^2.

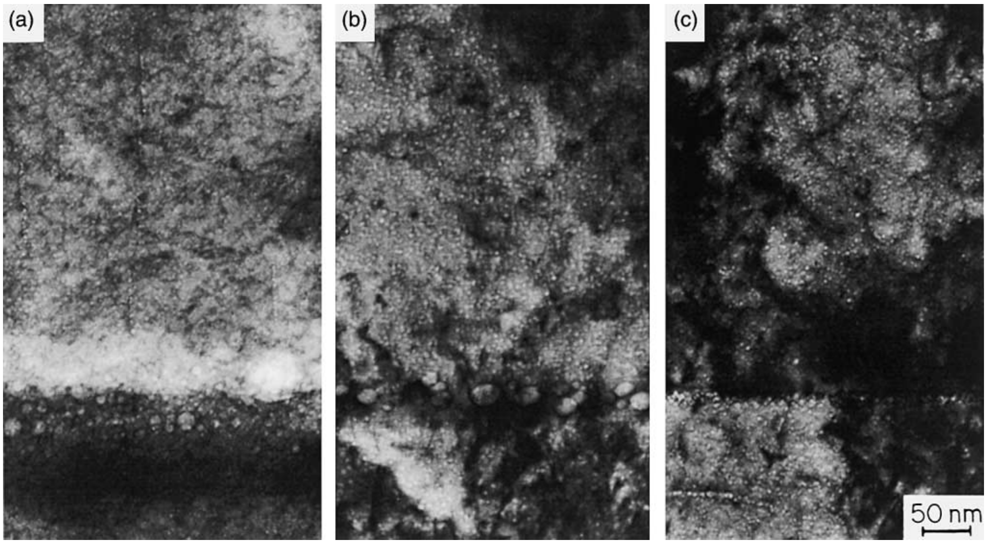

Fig. 5. Cavities formed in (a) Ni–9%Si, (b) Ni–5%Co and (c) Ni–5%Cu alloys irradiated at 500 °C by 25 keV He^+ ions to a dose of 4×10^{20} ions/m^2 under a flux of 5.6×10^{18} ions/m^2 s.

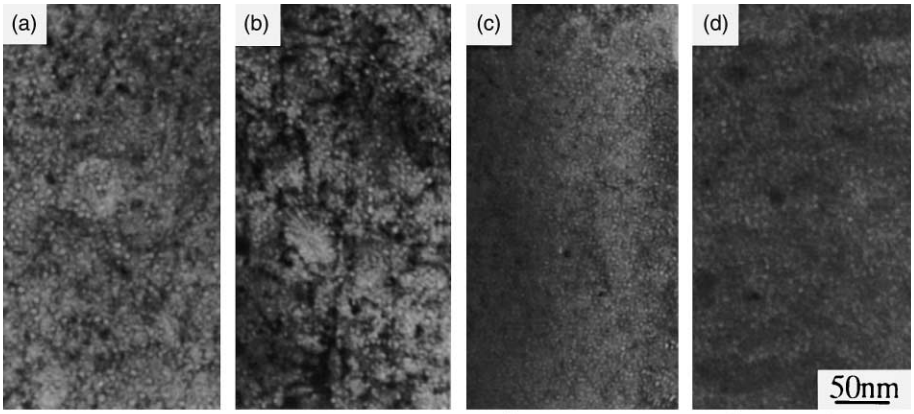

Ni Ni–5.0at%Si Ni–4.6at%Mn Ni–2.3at%Nb

Fig. 6. Cavities formed in (a) Ni, (b) Ni–5%Si, (c) Ni–5%Mn and (d) Ni–2%Nb alloys irradiated at 500 °C by 25 keV He^+ ions to a dose of 4×10^{20} ions/m^2 under a flux of 3.2×10^{18} ions/m^2 s.

defect production rate under electron irradiation, the density of dislocation loops formed in this study of He^+ irradiation was higher than that under electron irradiation. The dislocation loops formed by the electron irradiation have a dependence of solute atoms, but it hardly depended on the solute atoms under He^+ irradiation, except for the Ni–Si alloy. The results suggest that dislocation loops may be easily nucleate under He^+ irradiation through the formation of He–point defect complexes rather than di-interstitial and interstitial-solute complexes. The evolution of concentrations of interstitials, vacancies, interstital He atoms, the dislocation loops and bubbles under He^+ irradiation can be analyzed numerically by the following kinetic equations:

$$
\begin{aligned}
\mathrm{d}C_\mathrm{i}/\mathrm{d}t = {} & P\{1 - zC_\mathrm{v} - N_\mathrm{R}(C_\mathrm{gv} + C_\mathrm{2gv} + C_\mathrm{3gv} + C_\mathrm{4gv})\} \\
& - z(M_\mathrm{i} + M_\mathrm{v})C_\mathrm{i}C_\mathrm{v} - zM_\mathrm{i}C_\mathrm{i}(C_\mathrm{gv} + C_\mathrm{2gv} \\
& + 2C_\mathrm{i} + C_\mathrm{i3gv}) + zM_\mathrm{d}C_\mathrm{i3gv} - M_\mathrm{i}C_\mathrm{iziL}C_\mathrm{sL} \\
& + D_\mathrm{i}(\mathrm{d}^2C_\mathrm{i}/\mathrm{d}r^2),
\end{aligned}
$$

$$
\begin{aligned}
\mathrm{d}C_\mathrm{v}/\mathrm{d}t = {} & P(1 - zC_\mathrm{v}) - z(M_\mathrm{i} + M_\mathrm{v})C_\mathrm{i}C_\mathrm{v} - z(M_\mathrm{g} \\
& + M_\mathrm{v})C_\mathrm{g}C_\mathrm{v} - M_\mathrm{v}C_\mathrm{v}z_\mathrm{vL}C_\mathrm{sL} + zM_\mathrm{1d}C_\mathrm{gv} \\
& + D_\mathrm{v}(\mathrm{d}^2C_\mathrm{v}/\mathrm{d}r^2),
\end{aligned}
$$

$$\begin{aligned}\mathrm{d}C_{\mathrm{g}}/\mathrm{d}t = {} & P_{\mathrm{g}} + PN_{\mathrm{R}}(C_{\mathrm{gv}} + 2C_{2\mathrm{gv}} + 3C_{\mathrm{gv}} + 4C_{\mathrm{gv}}) \\ & + zM_{\mathrm{i}}C_{\mathrm{i}}(C_{\mathrm{gv}} + 2C_{2\mathrm{gv}}) + zM_{2\mathrm{d}}(C_{2\mathrm{gv}} + C_{3\mathrm{gv}}) \\ & - z(M_{\mathrm{g}} + M_{\mathrm{v}})C_{\mathrm{v}}C_{\mathrm{g}} - zM_{\mathrm{g}}C_{\mathrm{g}}(C_{\mathrm{gv}} + C_{2\mathrm{gv}} + C_{3\mathrm{gv}}) \\ & + D_{\mathrm{g}}(\mathrm{d}^2C_{\mathrm{g}}/\mathrm{d}r^2),\end{aligned}$$

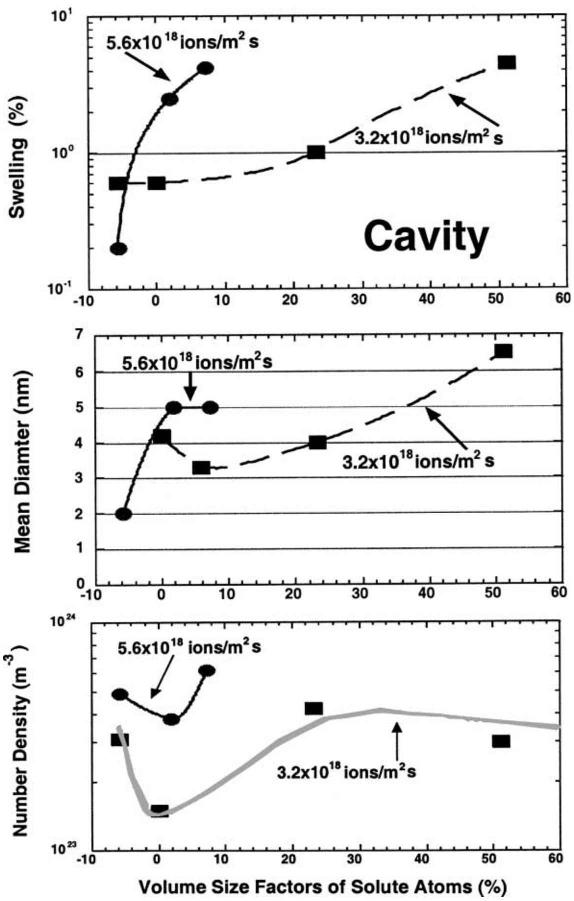

Fig. 7. Swelling, mean diameter and number density of cavities formed in Ni alloys and pure Ni irradiated by 25 keV He^+ ions.

$$\begin{aligned}\mathrm{d}C_{\mathrm{gv}}/\mathrm{d}t = {} & z(M_{\mathrm{g}} + M_{\mathrm{v}})C_{\mathrm{v}}C_{\mathrm{g}} - zM_{\mathrm{g}}C_{\mathrm{g}}C_{\mathrm{gv}} - zM_{\mathrm{i}}C_{\mathrm{i}}C_{\mathrm{gv}} \\ & - PN_{\mathrm{R}}C_{\mathrm{gv}} - zM_{1\mathrm{d}}C_{\mathrm{gv}} + zM_{2\mathrm{d}}C_{2\mathrm{gv}},\end{aligned}$$

$$\begin{aligned}\mathrm{d}C_{2\mathrm{gv}}/\mathrm{d}t = {} & zM_{\mathrm{g}}C_{\mathrm{g}}C_{\mathrm{gv}} - zM_{\mathrm{g}}C_{\mathrm{g}}C_{2\mathrm{gv}} - zM_{\mathrm{i}}C_{\mathrm{i}}C_{2\mathrm{gv}} \\ & - PN_{\mathrm{R}}C_{2\mathrm{gv}} + zM_{2\mathrm{d}}(-C_{2\mathrm{gv}} + C_{3\mathrm{gv}}),\end{aligned}$$

$$\begin{aligned}\mathrm{d}C_{3\mathrm{gv}}/\mathrm{d}t = {} & zM_{\mathrm{g}}C_{\mathrm{g}}C_{2\mathrm{gv}} - zM_{\mathrm{g}}C_{\mathrm{g}}C_{3\mathrm{gv}} - zM_{\mathrm{i}}C_{\mathrm{i}}C_{3\mathrm{gv}} \\ & - PN_{\mathrm{R}}C_{3\mathrm{gv}} + zM_{\mathrm{d}}C_{\mathrm{igv}} - zM_{2\mathrm{d}}C_{3\mathrm{gv}},\end{aligned}$$

$$\mathrm{d}C_{4\mathrm{gv}}/\mathrm{d}t = zM_{\mathrm{g}}C_{\mathrm{g}}C_{3\mathrm{gv}} - PN_{\mathrm{R}}C_{4\mathrm{gv}},$$

$$\mathrm{d}C_{\mathrm{i}3\mathrm{gv}}/\mathrm{d}t = zM_{\mathrm{i}}C_{\mathrm{i}}C_{3\mathrm{gv}} - PN_{\mathrm{R}}C_{4\mathrm{gv}},$$

$$\mathrm{d}C_{\mathrm{L}}/\mathrm{d}t = zM_{\mathrm{i}}C_{\mathrm{i}2} + zM_{\mathrm{i}}C_{\mathrm{i}}C_{\mathrm{i}3\mathrm{gv}},$$

$$\mathrm{d}C_{\mathrm{iL}}/\mathrm{d}t = C_{\mathrm{sL}}(z_{\mathrm{iL}}M_{\mathrm{i}}C_{\mathrm{i}} - z_{\mathrm{vL}}M_{\mathrm{v}}C_{\mathrm{v}}).$$

Here, C's denote the concentration of interstitials (C_{i}), vacancies (C_{v}), interstitial He atoms (C_{g}), He–vacancy clusters (C_{gv}), 2He–V clusters ($C_{2\mathrm{gv}}$), 3He–V clusters ($C_{3\mathrm{gv}}$), 4He–V clusters ($C_{4\mathrm{gv}}$), interstitial atoms with 3He–V clusters ($C_{\mathrm{i}3\mathrm{gv}}$), dislocation loops ($C_{\mathrm{L}}$), and interstitials in all of the dislocation loops (C_{iL}). M_{i}, M_{v}, M_{d}, $M_{1\mathrm{d}}$, $M_{2\mathrm{d}}$, P, P_{g}, N_{R} and z denote the mobility of interstitial, vacancy mobility, the dissociation rate of I–2He–V, He–V and 2He–V clusters, the production rate of Frenkel pairs, the injection rate of He atoms, the number of collision in a replacement collision sequence, and the capture site number of each reaction, respectively. The last equation shows the growth of interstitial loops [6]. In this model, there are some postulations that each He–vacancy cluster grows by absorbing a He atom and decomposes. In this calculation, the effect of the cascade on Frenkel pair production is ignored, because the averaged number of displacement atoms per cascade damage is calculated to be 2.5 by the Kinchin–Pease model in this He^+ irradiation. Fig. 9 shows that both of vacancy and interstitial concentrations are decreased

Table 2
The number density and mean size of interstitial-type dislocation loops in pure Ni and binary Ni alloys irradiated at 500 °C by He^+ ions with a dose of $1.0 \times 10^{19}\ \mathrm{m}^{-2}$

Specimen	V_{sf} (%)	Number density (m^{-3})	Mean size (nm)
Ni	0	1.5×10^{22}	19.5
Ni–Si	−5.7	2.3×10^{22}	13.2
Ni–Co	1.8	1.6×10^{22}	13.5
Ni–Cu	7.2	1.5×10^{22}	17.3
Ni–Mn	23.2	1.2×10^{22}	18.2
Ni–Pd	43.3	1.4×10^{22}	18.9
Ni–Nb	51.2	1.3×10^{22}	16.8

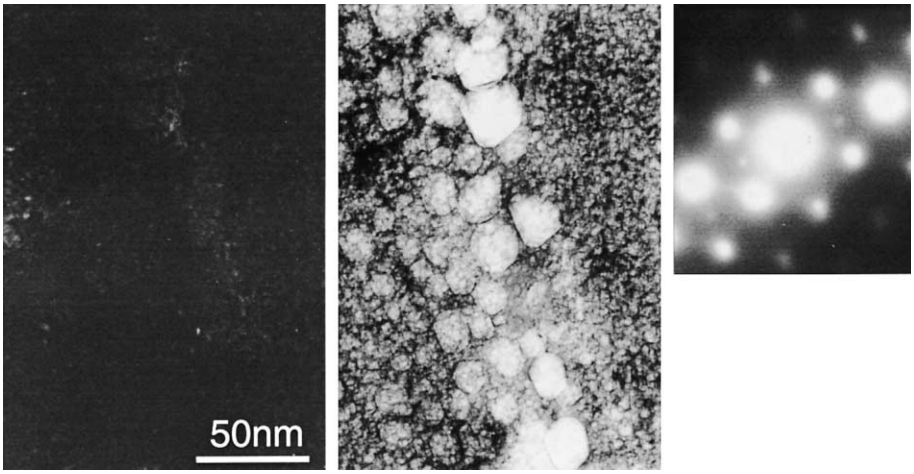

Fig. 8. Ni_3Si precipitates formed on the surface of cavities in matrix and around grain boundary in Ni–9Cr alloys irradiated at 500 °C by 25 keV He^+ ions to a dose of 4×10^{20} ions/m^2 (a) dark-field image of Ni_3Si precipitates, (b) bright-field image, (c) diffraction pattern.

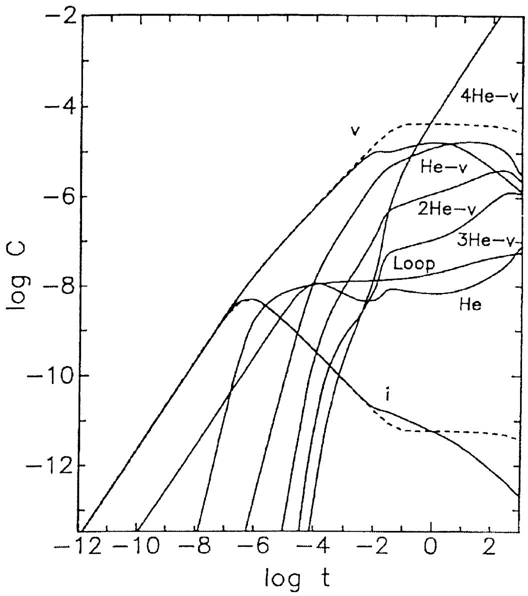

Fig. 9. The calculated concentrations of interstitials, vacancies, interstitial He, He–vacancy clusters (He–V, 2He–V, 3He–V, 4He–V), and dislocation loops against the logarithm of irradiation time in Ni irradiated by 25 keV He^+ ions (solid line) of 5.46×10^{18} ions/m^2 s and by 2 MeV electrons (broken lines) at 500 °C. Parameters are described as below: 0.15, 1.2 and 0.6 eV for the migration of interstitials, vacancies and interstitial He, respectively, 0.75, 1.9 and 1.7 eV for the dissociation of I–3He–V, He–V and 2He–V clusters, respectively, $N_R = 10$ and $z = 81$.

under the He irradiation, compared with the electron irradiation. This is explained qualitatively as follows: the vacancy concentration was decreased by the strong interaction of an interstitial He atom with He–V clusters, and the interstitial concentration was decreased by the absorption of interstitials to higher density dislocation loops. The cause of the formation of the high density of dislocation loops might be induced by the formation of He–point defect complexes under He irradiation.

The number density of bubbles tended to increase with it. The cause of the enhancement of bubble formation may be owing to the reduction of the mobility of He atoms or vacancies in Ni alloys. It is known that He atoms migrate in a dissociative mechanism in which the He atoms jump out from their substitutional positions and migrate interstitially; i.e., from He–V complex to interstitial He atom and vacancy. In Ref. [7], the vacancy mobility in Ni alloys was not necessarily reduced with increasing the volume size of solute atoms i.e., the migration energies of pure Ni, Ni–Si, Ni–Co, Ni–Cu, Ni–Mn, Ni–Pd and Ni–Nb were 1.20, 1.35, 1.26, 1.65, 1.08, 1.0 and 0.92 eV, respectively. Therefore, it is suggested that the mobility of interstitial He atoms may be somewhat suppressed by solute atoms, and the formation of bubbles may be enhanced with the solute volume size.

As shown in Table 3, the mean diameter of dislocation loops in the Ni alloys increased with the volume size factors, and the vacancy concentration in the alloys with larger volume size factor of solute atom may be higher than that in the alloys with the smaller size factor. On the other hand, the vacancy mobility in Ni alloys tended to decrease inversely with the larger volume size factors in Ni [7]. Therefore, the swelling in Ni alloys would tend to increase with the volume size factors of solute atoms.

Table 3
The number density and mean size of bubbles and the swelling in pure Ni and binary Ni alloys irradiated at 500 °C by He^+ ions with a dose of 4.1×10^{20} m^{-2}. V_{sf} is the volume size factors of solute in Ni

Specimen	V_{sf} (%)	Flux (He^+/m^2 s)	Number density (m^{-3})	Mean size (nm)	Swelling (%)
Ni–Si	−5.8	5.6×10^{18}	4.9×10^{23}	2.0	0.2
Ni–Co	1.8	5.6×10^{18}	3.8×10^{23}	5.0	2.5
Ni–Cu	7.2	5.6×10^{18}	6.2×10^{23}	5.0	4.2
Ni	0	3.2×10^{18}	1.5×10^{23}	4.2	0.6
Ni–Si	−5.8	3.2×10^{18}	3.1×10^{23}	3.3	0.6
Ni–Mn	23.2	3.2×10^{18}	4.2×10^{23}	4.0	1.0
Ni–Nb	51.2	3.2×10^{18}	3.0×10^{23}	6.5	4.5

5. Conclusion

The effects of solute atoms on the microstructural evolution have been investigated using Ni alloys under 25 keV He^+ irradiation at 500 °C. The specimens used were pure Ni, Ni–Si, Ni–Co, Ni–Cu, Ni–Mn and Ni–Pd alloys, and these volume size factors of solute atoms in Ni are −5.8%, +1.8%, +7.2%, +23.2%, +41.3% and +51.2%, respectively. The high number densities of dislocation loops of about 1.5×10^{22} m^{-3} were formed in the specimens irradiated to 1×10^{19} ions/m^2, and they were approximately equivalent, except for Ni–Si. The mean size of loops tended to increase with the volume size factor of solute atoms. In a dose of 4×10^{20} ions/m^2, the swelling changed from 0.2% to 4.5%, depending on the volume size factors. The number densities of bubbles tended to increase with the volume size factor, but the mean size of the cavity also increased with the volume size factors. This result suggests that the mobility of helium and vacancy atoms may be influenced by the interaction of solute atoms with them.

Acknowledgements

The authors would like to thank Professor Nasu of Osaka University for a useful discussion in this study.

References

[1] T. Ezawa, E. Wakai, R. Oshima, J. Nucl. Mater. 283–287 (2000) 244.
[2] E. Wakai, T. Ezawa, T. Tanabe, R. Oshima, Mater. Trans. JIM 33 (1992) 884.
[3] T. Yoshiie, Q. Xu, Y. Satoh, H. Ohkubo, M. Kiritani, J. Nucl. Mater. 283–287 (2000) 229.
[4] K. Niwase, T. Ezawa, F.E. Fujita, H. Kusanagi, H. Takaku, Radiat. Eff. 106 (1988) 65.
[5] H.W. King, J. Mater. Sci. 1 (1966) 79.
[6] M. Kiritani, H. Takata, J. Nucl. Mater. 69&70 (1978) 277.
[7] E. Wakai, Radiation effects of Ni binary alloys under gas ion irradiation, Doctor thesis, Osaka University, 1993.